Dynamics of the roll and streak structure in transition and turbulence

By B. F. Farrell†, D. F. Gayme‡, P. J. Ioannou¶, B. K. Lieu††, AND M. R. Jovanović††

The prominence of streamwise elongated structures in wall-bounded shear flow turbulence previously motivated turbulence investigations using streamwise constant (2D/3C) and streamwise averaged (SSST) models. Results obtained using these models imply that the statistical mean turbulent state is in large part determined by streamwise constant structures, particularly the well studied roll and streak. In this work the role of streamwise structures in transition and turbulence is further examined by comparing theoretical predictions of roll/streak dynamics made using 2D/3C and SSST models with DNS data. The results confirm that the 2D/3C model accurately obtains the turbulent mean velocity profile despite the fact that it only includes one-way coupling from the cross-stream perturbations to the mean flow. The SSST system augments the 2D/3C model through the addition of feedback from this streamwise constant mean flow to the dynamics of streamwise varying perturbations. With this additional feedback, the SSST system supports a perturbation/mean flow interaction instability leading to a bifurcation from the laminar mean flow to a self-sustaining turbulent state. Once in this self-sustaining state the SSST collapses to a minimal representation of turbulence in which a single streamwise perturbation interacts with the mean flow. Comparisons of DNS data with simulations of this self-sustaining state demonstrate that this minimal representation of turbulence produces accurate statistics for both the mean flow and the perturbations. These results suggest that SSST captures fundamental aspects of the mechanisms underlying transition to and maintenance of turbulence in wall-bounded shear flows.

1. Introduction

The dynamical significance of streamwise elongated structures in wall-turbulence is supported by a growing body of work pointing to their central role in both transition to turbulence (Klebanoff *et al.* 1962; Andersson *et al.* 1999; Jovanović & Bamieh 2005) and maintenance of a turbulent flow (Jiménez & Moin 1991; Hamilton *et al.* 1995; Jiménez & Pinelli 1999). Streamwise coherent "roll cells" associated with streamwise elongated regions of low and high streamwise momentum have been observed in both Direct Numerical Simulations (DNS) of turbulent channel flow (Kim *et al.* 1987) as well as in boundary layer and pipe flow experiments (Kim & Adrian 1999; Morrison *et al.* 2004; Guala *et al.* 2006; Hutchins & Marusic 2007*a*). These so-called streak structures are of great interest because they account for a substantial portion of the turbulent kinetic energy (Morrison *et al.* 2004; Hutchins & Marusic 2007*a*,*b*) and have been shown to modulate the activity of near-wall structures (Hutchins & Marusic 2007*b*; Mathis *et al.* 2009).

† Department of Earth and Planetary Sciences, Harvard University
‡ Department of Mechanical Engineering, Johns Hopkins University
¶ Department of Physics, National and Kapodistrian University of Athens
†† Department of Electrical and Computer Engineering, University of Minnesota

The importance of these streamwise coherent structures previously motivated the use of a streamwise constant (so-called 2D/3C) model for plane Couette flow, which was shown to accurately simulate the mean turbulent velocity profile (Gayme *et al.* 2010). A more comprehensive model can be obtained by including feedback from the streamwise constant mean flow to the dynamics of the perturbation field. A recent parameterization of this feedback was incorporated in a Stochastic Structural Stability Theory (SSST) model using a second order closure (Farrell & Ioannou 2012).

In both the 2D/3C and SSST models the flow field is decomposed into a streamwise constant mean flow and a streamwise varying perturbation field but they differ in their parameterizations of the perturbations. In the 2D/3C model, stochastically forced streamwise roll structures produce Reynolds stresses that drive the mean flow. The SSST model uses a three dimensional stochastic turbulence model (STM) along with an ensembling assumption to parameterize the perturbation dynamics. The associated Reynolds stresses force the streamwise roll structures and drive the mean flow, which is then used in the STM to evolve a consistent perturbation field. With these additions to the basic 2D/3C system, the SSST model produces both the mean turbulent velocity profile and the quadratic turbulence statistics. In addition, the inclusion of streamwise varying components and the feedback mechanisms associated with them enables the SSST system to capture both transition to turbulence and the self-sustaining process (SSP) that maintains the turbulent state (Farrell & Ioannou 2012). The success of these models in simulating turbulence statistics has implications for understanding the dynamics of turbulent flows. The 2D/3C model suggests that turbulence statistics are fundamentally determined by the streamwise invariant dynamics of the roll structure. The SSST model supports this notion and also implies that transition is instigated through an interaction instability. It further suggests that turbulence is maintained by an essentially non-normal, parametric, quasi-linear interaction instability regulated by a quasi-linear feedback process that determines the statistical mean state. In the current work, we test the validity of the mechanisms suggested by these models by comparing 2D/3C and SSST based simulations to DNS data. We begin by deriving a so-called quasi-linear (QL) numerical approximation of the SSST model from the Navier Stokes equations. The 2D/3C model is shown to be a simplification of the QL. We then discuss the underlying theory of these models and derive the full SSST dynamics. Finally, we compare results predicted by SSST (obtained from simulations of QL) and 2D/3C simulations to DNS data.

2. Modeling framework

Consider an incompressible unit density fluid in a channel and decompose the velocity fields as $\vec{u}_{tot} = \vec{u} + \vec{U}$, where the streamwise constant mean flow variables are denoted by uppercase letters and variables associated with perturbations from this mean flow are denoted by lowercase letters. Throughout this paper, streamwise averaged, spanwise averaged and ensemble averaged quantities are respectively denoted by an overbar, $\bar{\cdot}$, square brackets, $[\cdot]$ and angled brackets, $\langle\cdot\rangle$. Using these notations, the equations governing the mean flow and the perturbation fields are:

$$\vec{u}_t + \vec{U}\cdot\nabla\vec{u} + \vec{u}\cdot\nabla\vec{U} + \nabla p - \Delta\vec{u}/R = -(\vec{u}\cdot\nabla\vec{u} - \overline{\vec{u}\cdot\nabla\vec{u}}) + \vec{\epsilon}, \tag{2.1a}$$

$$\vec{U}_t + \vec{U}\cdot\nabla\vec{U} + \nabla P - \Delta\vec{U}/R = -\overline{\vec{u}\cdot\nabla\vec{u}}, \tag{2.1b}$$

$$\nabla\cdot\vec{u} = 0 \quad , \quad \nabla\cdot\vec{U} = 0, \tag{2.1c}$$

where the Reynolds number (R) is the only explicit parameter. The term $\vec{\epsilon}$ in (2.1a) represents an externally imposed stochastic forcing. In a DNS this $\vec{\epsilon}$ typically represents the initial condition required to instigate transition to turbulence. In the current work it represents a small finite time stochastic disturbance that is used in a similar manner. In what follows, we refer to the system (2.1) as the NL system.

We first simplify (2.1) by stochastically parameterizing both the perturbation-perturbation nonlinearity ($\vec{u}\cdot\nabla\vec{u}-\overline{\vec{u}\cdot\nabla\vec{u}}$) and the external excitation in equation (2.1a) to obtain

$$\vec{u}_t+\vec{U}\cdot\nabla\vec{u}+\vec{u}\cdot\nabla\vec{U}+\nabla p-\Delta\vec{u}/R=\vec{e}, \tag{2.2a}$$

$$\vec{U}_t+\vec{U}\cdot\nabla\vec{U}+\nabla P-\Delta\vec{U}/R=-\overline{\vec{u}\cdot\nabla\vec{u}}, \tag{2.2b}$$

where $\vec{e}$ is a stochastic forcing to be specified. This is a nonlinear system where the first equation (2.2a) captures interactions between the streamwise constant mean flow $\vec{U}$ and the streamwise varying perturbations $\vec{u}$. The mean flow equation (2.2b) is driven by the streamwise constant component of the Reynolds stresses, $\overline{\vec{u}\cdot\nabla\vec{u}}$. Hereafter, the equations (2.2) will be referred to as the QL system.

The mean flow considered here consists of streamwise, U, wall-normal, V, and spanwise, W, velocity components. The nondivergence of this velocity field can be enforced by defining a stream function Ψ that satisfies $V=-\Psi_z$, $W=\Psi_y$. For non-zero V and W the mean flow has a roll structure, with mean streamwise vorticity $\Omega_x=\Delta_1\Psi$, where $\Delta_1\equiv\partial^2_{xx}+\partial^2_{zz}$. The deviation of the streamwise velocity $U(y,z,t)$ from its spanwise average $[U](y,t)$ defines the streak velocity $U_s(y,z,t)$. In terms of the streamwise mean velocity U and the stream function Ψ the mean equation (2.2b) takes the form

$$U_t-U_y\Psi_z+U_z\Psi_y-\Delta_1U/R=F^x, \tag{2.3a}$$

$$\Delta_1\Psi_t-(\partial_{yy}-\partial_{zz})\Psi_y\Psi_z+\partial_{yz}(\Psi^2_y-\Psi^2_z)-\Delta_1\Delta_1\Psi/R=F^{yz}, \tag{2.3b}$$

$$F^x=-\partial_y\overline{uv}-\partial_z\overline{uw},\qquad F^{yz}=-(\partial_{yy}-\partial_{zz})\overline{vw}-\partial_{yz}(\overline{w^2}-\overline{v^2}). \tag{2.3c}$$

The streamwise mean velocity, U, in (2.3a) is forced by the Reynolds stress divergence F^x, which is obtained from (2.2a) and by $U_y\Psi_z-U_z\Psi_y$, the first part of which is the familiar lift-up mechanism. The Reynolds stress term in (2.3b), F^{yz}, provides the streamwise roll forcing by generating streamwise mean vorticity, $\Omega_x=\Delta_1\Psi$. The mean velocities can only advect Ω_x, via the term $-(\partial_{yy}-\partial_{zz})\Psi_y\Psi_z+\partial_{yz}(\Psi^2_y-\Psi^2_z)$.

A minimal 2D/3C representation of (2.3) is obtained by setting $F^x=0$ in (2.3a) and parameterizing F^{yz} in (2.3b) as a stochastic excitation as follows:

$$U_t-U_y\Psi_z+U_z\Psi_y-\Delta_1U/R=0, \tag{2.4a}$$

$$\Delta_1\Psi_t-(\partial_{yy}-\partial_{zz})\Psi_y\Psi_z+\partial_{yz}(\Psi^2_y-\Psi^2_z)-\Delta_1\Delta_1\Psi/R=F_L(y,z,t). \tag{2.4b}$$

In the simulations described in Section 6, the stochastic excitation $F_L(y,z,t)$ in (2.4b) is generated by the Reynolds stresses obtained by stochastically forcing the perturbation dynamics linearized about a laminar Couette flow. A similar stochastic forcing is used to force the perturbation field in the QL simulations, except that the Reynolds stresses arise from linearizing about the time dependent mean flow $\vec{U}$.

Figure 1 illustrates the nonlinear interactions between the mean flow and perturbation dynamics that are captured by the 2D/3C and QL models. Both of these models include pathway (1) in which the perturbations ($\vec{u}$) influence the dynamics of the mean flow ($\vec{U}$). However, the QL (and its associated ensemble mean SSST model) also includes the feedback pathway (2), from the mean flow to the perturbation dynamics.

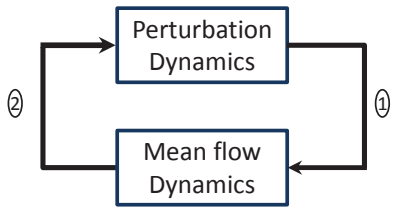

FIGURE 1. In both the 2D/3C (2.4) and QL (2.2) (and its associated ensemble mean SSST model) the perturbations ($\vec{u}$) influence the dynamics of the mean flow ($\vec{U}$). This coupling is denoted pathway (1) in the block diagram. The SSST model augments the 2D/3C formulation with feedback from the mean flow to the perturbation dynamics, which is illustrated through pathway (2).

3. Relation of 2D/3C and QL to SSST

The QL and the 2D/3C models are stochastic dynamical systems. Theoretical understanding of the behavior of these systems is facilitated by considering the dynamics of the associated ensemble mean systems. The ensemble mean dynamical system associated with QL is the SSST system, which is given explicitly by equation (3.3) below. The SSST system comprises the streamwise mean flow dynamics coupled to the second order covariances of the flow fields obtained using a stochastic turbulence model. The SSST is preferred for theoretical investigations because it is a second order closure in which quadratic perturbation quantities are directly computed in terms of the perturbation covariance, which is the perturbation variable in SSST.

An analytically and computationally powerful simplification used in the derivation of the SSST system is to equate the ensemble means of second order perturbation statistics with the streamwise average of these quantities. In this way, the ensemble mean of a Reynolds stress can be assumed to be equal to the streamwise mean of that Reynolds stress.

We write the stochastically forced perturbation equation (2.2a) concisely as

$$\partial_t \phi = \mathsf{A}\phi + e, \tag{3.1}$$

where A is the dynamical operator linearized about the instantaneous mean flow $\vec{U}$. A governs the evolution of the perturbation state ϕ. If we define the covariance of the perturbation fields between coordinate point a and b as $C(a,b) =< \phi(a)\phi(b) >$ where $\phi(a)$ is any perturbation state at point a (similarly for b), and multiply the perturbation equations (3.1) at locations a and b with $\phi(b)$ and $\phi(a)$ respectively we obtain the following ensemble mean covariance equation

$$\partial_t \mathsf{C}(a,b) = (\mathsf{A}(a) + \mathsf{A}(b))\mathsf{C}(a,b) + \mathsf{Q}(a,b). \tag{3.2}$$

Here, $\mathsf{Q}(a,b)$ is the spatial covariance of the forcing, defined as: $< e(a,t_1)e(b,t_2) >:= \delta(t_1-t_2)\mathsf{Q}(a,b)$. The spatial covariance of this forcing will be assumed to be homogeneous. The operator $\mathsf{A}(a)$ acts only on the $\phi(a)$ component of $\mathsf{C}(a,b)$ and similarly $\mathsf{A}(b)$ acts only on the $\phi(b)$ component. With this notation, all of the Reynolds stress terms in (2.3c) can be expressed in terms of C. For example,

$$\partial_y < uv >= \partial_y \left\langle u(a)v(b)\right\rangle\big|_{a=b} = \left(\partial_{y(a)} + \partial_{y(b)}\right) \mathsf{C}_{uv}(a,b)\big|_{a=b},$$

where $\mathsf{C}_{uv}(a,b) =< u(a)v(b) >$. In this way we obtain the autonomous and deterministic

SSST system that governs the evolution of the mean flow (U, Ψ) and the perturbation field expressed in terms of its covariance field C. The SSST system is then

$$\partial_t \mathsf{C}(a,b) = (\mathsf{A}(a) + \mathsf{A}(b))\mathsf{C}(a,b) + \mathsf{Q}(a,b), \tag{3.3a}$$

$$U_t - U_y\Psi_z + U_z\Psi_y - \Delta_1 U/R = \langle F_x \rangle\,, \tag{3.3b}$$

$$\Delta_1\Psi_t - (\partial_{yy} - \partial_{zz})\Psi_y\Psi_z + \partial_{yz}(\Psi_y^2 - \Psi_z^2) - \Delta_1\Delta_1\Psi/R = \langle F_{yz} \rangle\,. \tag{3.3c}$$

The corresponding ensemble mean Reynolds stress divergences are obtained from the perturbation covariance as

$$\langle F_x \rangle = -\left[\left(\partial_{y(a)} + \partial_{y(b)}\right)\mathsf{C}_{uv}(a,b) + \left(\partial_{z(a)} + \partial_{z(b)}\right)\mathsf{C}_{uw}(a,b)\right]_{a=b}, \tag{3.4a}$$

$$\begin{aligned}\langle F_{yz} \rangle = &-\left[\left(\left(\partial_{y(a)} + \partial_{y(b)}\right)^2 - \left(\partial_{z(a)} + \partial_{z(b)}\right)^2\right)\mathsf{C}_{vw}(a,b)\right]_{a,b} \\ &-\left[\left(\partial_{y(a)} + \partial_{y(b)}\right)\left(\partial_{z(a)} + \partial_{z(b)}\right)\left(\mathsf{C}_{ww}(a,b) - \mathsf{C}_{vv}(a,b)\right)\right]_{a=b}.\end{aligned} \tag{3.4b}$$

The counterpart of the SSST system in this work is the QL model (2.2). The QL also employs a stochastic parameterization of perturbation-perturbation interaction and exploits the streamwise mean flow and perturbation decomposition to obtain quasi-linear dynamics. However, in QL the perturbation covariance is not solved for directly and no large ensemble approximation is made. The advantage of QL is that it can be directly simulated in a manner that is computationally feasible for large systems, through a restriction of a DNS code to the QL dynamics of (2.2). The SSST model, which has the perturbation covariance as a variable, has dimension $\mathrm{O}(N^2)$ for a system of dimension $\mathrm{O}(N)$ and is only directly integrable for low order systems. In this work we compare predictions based on previous low order simulations of the SSST (Farrell & Ioannou 2012) to a higher order QL simulation, a 2D/3C model and DNS data.

4. Analysis of the models and prior results

We study Couette flow and define the Reynolds number R based on the wall velocities $\pm U_c$ and the channel half width h. In the absence of forcing, both the 2D/3C model (2.4) and the SSST model (3.3) admit the laminar Couette flow as an equilibrium. This solution is globally stable for the unforced 2D/3C model (Gayme 2010), which implies that this system will return to the laminar Couette flow if the forcing is removed. A stochastically forced 2D/3C model captures the turbulent mean flow profile, as shown in Figure 2. The mechanisms underlying maintenance of this mean flow profile are further described in Gayme (2010). Although the 2D/3C model captures the basic dynamics of the interaction between rolls and the mean turbulent velocity profile, it does not include the feedback from the mean flow to the perturbation dynamics (as seen in Figure 1). As described below, this feedback is critical for capturing the mechanism of transition and the establishment of the self-sustaining process that maintains the turbulent state.

At fixed R and with sufficiently small values of forcing, the SSST model has a globally stable equilibrium state with a streamwise mean component that varies only in the wall-normal direction (i.e. there is no roll or streak). As the forcing increases, this equilibrium bifurcates and at sufficiently high forcing a saddle-node bifurcation occurs. At this point the SSST flow becomes time dependent and has the mean structure and perturbation statistics of fully turbulent Couette flow. As described in Farrell & Ioannou (2012), transition to turbulence in SSST is associated with this perturbation/mean flow interaction instability. During transition to the time-dependent SSST state, evolution under SSST produces the familiar overshoot of flow quantities that occurs before the flow settles onto

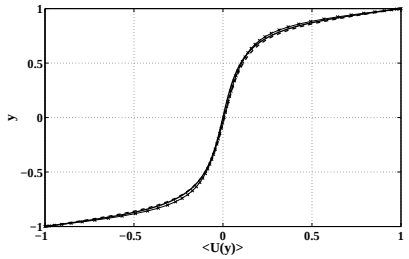

FIGURE 2. Turbulent mean velocity profiles (based on a streamwise, spanwise and time averages) obtained from DNS with the $L_x = 4\pi$ channel (solid line), the QL model (line with an x marker) and the 2D/3C model (dashed line), all at R=1000. The forcing f in the 2D/3C model is 0.065. There is no forcing applied to the DNS or QL during the time interval used to generate the profile, (i.e. the QL is in the self-sustaining state).

the turbulent attractor. After transition to turbulence the forcing can be removed and the turbulence self-sustains, with little change in the turbulence statistics. In a minimal channel with no forcing, the SSST perturbation covariance collapses to rank 1 with the perturbation field becoming asymptotically confined to a single streamwise component during the self sustaining state. The SSST framework therefore suggests that the interaction of a perturbation field at a single streamwise wave number with the mean flow provides a minimal representation of turbulent Couette flow (Farrell & Ioannou 2012).

5. Numerical approach

The numerical simulations in this paper are based on a spectral code developed by Gibson (2012). The time integration uses a third order multistep semi-implicit Adams-Bashforth/backward-differentiation scheme that is detailed in Peyret (2002). The discretization time step is automatically adjusted such that the Courant-Friedrichs-Lewy (CFL) is kept between 0.05 and 0.2. The spatial derivatives employ Chebyshev polynomials in the wall-normal (y) direction and Fourier series expansions in the streamwise (x) and spanwise (z) directions (Canuto *et al.* 1988). No-slip boundary conditions in the wall-normal direction and periodic boundary conditions in the streamwise (x) and spanwise (z) directions are imposed on the velocity fields. Aliasing errors from the evaluation of the nonlinear terms are removed by the 3/2-rule when the horizontal FFTS are computed, as detailed in Zang & Hussaini (1985). A zero constant pressure gradient was imposed in all simulations.

We employ two different computational boxes for the DNS. The lengths of the first computational box in units of channel half height h are $L_x = 4\pi$, $y \in [-1, 1]$ and $L_z = 4\pi$ with $N_x \times N_y \times N_z = 128 \times 65 \times 128$ grid points in the x, y and z directions. The second DNS box represents a minimal channel in the streamwise direction (Jiménez & Moin 1991) with $L_x = 1.2\pi$ and $N_x = 64$. In order to perform the QL and $2D/3C$ computations the DNS code was respectively restricted to the dynamics of (2.2) and (2.4).

The stochastic forcing for all of the models was constructed by first creating independent random excitations of the streamwise and wall-normal velocities. These were used to derive the spanwise excitation that produces a divergence free flow. For the $L_x = 1.2\pi$ simulations the stochastic forcing was designed to only excite the streamwise mode with a wave number of $k_x = 1.67$, which is the largest streamwise harmonic perturbation in the $L_x = 1.2\pi$ channel. The structure of the random excitations of the streamwise and

wall-normal momentum equations are given by

$$\Xi(x,y,z) \;=\; 2W(\alpha,y)\sum_{n=-M_z/2}^{M_z/2}\sum_{m=0}^{M_y}\mathrm{Re}\left(a_{mn}\,e^{2\pi\mathrm{i}(x/L_x+nz/L_z)}\right)T_m(y), \tag{5.1}$$

where $T_m(y)$ is the m^{th} Chebyshev polynomial. The number of modes excited in y and z are $M_y = (1/2)N_y$ and $M_z = (2/3)N_z$. We use a Tukey window function $W(\alpha, y)$ with $\alpha = 0.4$ in order to obtain smooth forcing realizations close to the walls. The coefficients a_{mn} are complex random numbers that are normally distributed with zero mean and variance 2. These numbers are regenerated every $\Delta T = 0.05$. If the normalized forcing obtained from the random Ξ that satisfies $\|\vec{\mathcal{F}}\|_2^2 = 1$ (i.e. has a unit energy norm) is denoted by $\vec{\mathcal{F}}$, then the body force introduced every ΔT is $\vec{F} = f/\sqrt{\Delta T}\;\vec{\mathcal{F}}$. We divide this forcing by $\sqrt{\Delta T}$ so that its variance is independent of ΔT. The parameter f controls the amplitude of the forcing and is an adjustable parameter in the simulations.

6. Results

In this section we compare 2D/3C and QL simulations to DNS. Figure 2 demonstrates a close correspondence between the mean velocity profiles resulting from 2D/3C, QL, and DNS simulations. Further results obtained using the SSST and 2D/3C model were previously reported in Farrell & Ioannou (2012) and Gayme *et al.* (2010). Here we focus on the roll and streak structure and the dynamical properties of the flow field. All simulations in this section were conducted at $R = 1000$.

Figure 3 compares QL, 2D/3C and DNS RMS streak, $\sqrt{U_s^2}$, roll, $\sqrt{V^2+W^2}$, and perturbation, $\sqrt{u^2+v^2+w^2}$, velocities along with the square root of the change in their energy from that of the laminar flow. Figure 3(d) shows that the RMS of the change from the laminar velocity obtained in the QL simulation and the DNS are very similar, whereas the 2D/3C produces slightly more energy. This additional energy is primarily a result of the larger RMS streak velocity seen in Figure 3(a). However, the RMS perturbation velocity ($\sqrt{u^2+v^2+w^2}$) in the 2D/3C simulation is less than that of both the QL and DNS, as shown in Figure 3(c). This result is consistent with the fact that in the 2D/3C the streak is not regulated by feedback from the mean flow to the perturbation field, pathway (2) in Figure 1. This regulation corrects the streak in the QL model to a value similar to that of the DNS.

The forcing in the QL simulation shown in Figure 3 was stopped at $t = 500$, which indicates that the behavior of the QL for $t > 500$, which is similar to that of the DNS, is a result of the self-sustaining process (SSP) described in Farrell & Ioannou (2012). This behavior is further explored in Figure 4, which shows the time evolution of turbulent statistics obtained by continuing the QL beyond $t = 500$ with the following three different levels of forcing: $f = 0$, $f = 0.04$ and $f = 0.1$. The fact that the amount of forcing applied to the QL after $t = 500$ had minimal effect on the turbulence seen in Figure 4 indicates that the turbulent state in the self-sustaining regime is tightly regulated by the two-way coupling in the QL.

Figures 5(a) and 5(b) show details of roll and streak development during transition and establishment of the turbulent state for DNS, QL and 2D/3C. Here, the effect of feedback from the mean flow to the perturbations, pathway (2) in Figure 1, is quite evident. Lack of this feedback in 2D/3C results in the streak continuing to grow after the transient growth phase. In QL and DNS, the magnitude of the streak is reduced through a combination

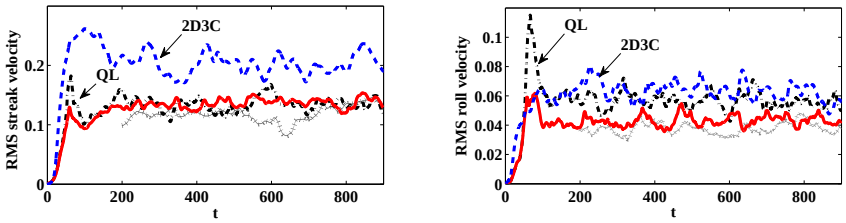

(a) RMS streak velocity (b) RMS roll velocity

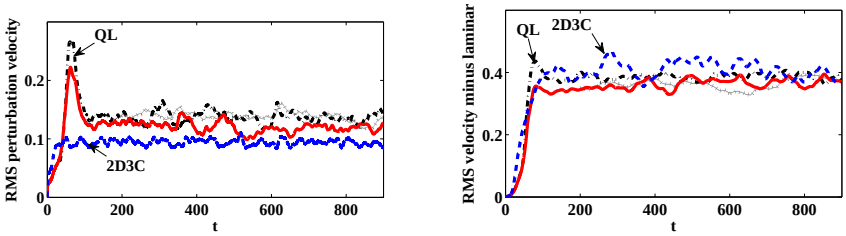

(c) RMS perturbation velocity (d) RMS departure from laminar velocity

FIGURE 3. Roll, streak and perturbation development during transition and turbulence at $R = 1000$. Shown are (a) RMS streak velocity $\sqrt{U_s^2}$, (b) RMS roll velocity $\sqrt{V^2 + W^2}$, (c) RMS perturbation velocity $\sqrt{u^2 + v^2 + w^2}$, and (d) RMS velocity departure from the laminar flow. All figures show DNS for boxes with $L_x = 1.2\pi$ (solid line) and $L_x = 4\pi$ (cross-marker with line), QL forced with $f = 0.04$ at $k_x = 1.67$ (dash-dot line) and the 2D/3C with $f = 0.04$ (dashed line). The perturbation forcing of the QL simulation was stopped at $t = 500$ demonstrating that after transition, the QL self-sustains.

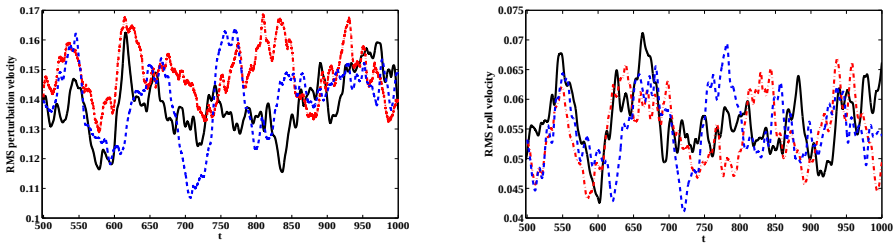

FIGURE 4. The self sustaining state in the QL simulation. In all plots the QL was forced with amplitude $f = 0.04$ until $t = 500$. At $t = 500$ the same QL was evolved under no forcing $f = 0$ (solid), with $f = 0.04$ (dashed) and with $f = 0.1$ (dashed-dot). Shown are (left) the RMS perturbation velocity $\sqrt{u^2 + v^2 + w^2}$ and (right) the RMS roll velocity $\sqrt{V^2 + W^2}$. This shows that after the QL enters the self sustaining state, the statistics are independent of f. When the QL is on this turbulent attractor the dynamics are strongly regulated by the interaction between the perturbations and the roll/streak structure.

of perturbation Reynolds stress induced dissipation and modification to the roll forcing based on feedback from the mean flow. Another feature of Figure 5 is the prominent initial overshoot of roll and streak energy that occurs just prior to the establishment of a statistically steady turbulent state in the QL and DNS. This overshoot is associated with the perturbation/mean flow structural instability described in Farrell & Ioannou (2012). The exponential growth of this instability is intercepted by nonlinear feedback dynamics that regulate the unstable growth and establishes the statistically steady turbulent state. This agrees with the dynamics predicted by the low order minimal channel simulation of

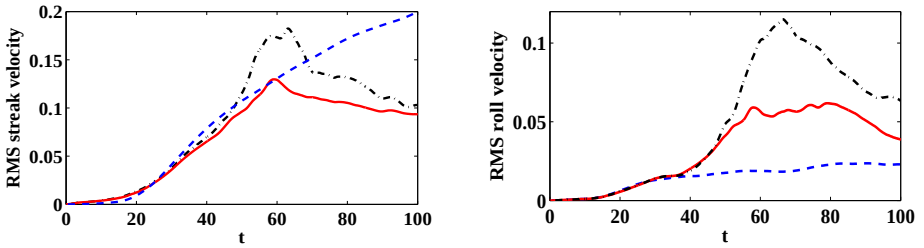

(a) Streak development (b) Roll development

FIGURE 5. Initial development of the roll and streak structure during transition to turbulence at $R = 1000$. Shown are the RMS values of (a) the streak velocity $\sqrt{U_s^2}$ and (b) the roll velocity $\sqrt{(V^2 + W^2)}$ for DNS (solid line), QL (dashed-dot), 2D/3C (dashed line). All simulations were initialized from a laminar state. A stochastic perturbation forcing with amplitude $f = 0.04$ was introduced to instigate transition. This figure shows that the QL and DNS exhibit exponential growth of the roll/streak structure in accordance with the roll/streak instability predicted by SSST with the predicted overshoot and subsequent establishment of the feedback regulated turbulent state. The 2D/3C produces continued algebraic growth of the roll/streak structure because of the lack of feedback from the mean flow to the perturbations, pathway (2) in Figure 1.

SSST shown in Figure 24 of Farrell & Ioannou (2012) and serves to validate the SSST theory first introduced in that work.

Figure 6 shows contour plots of the U velocity field superimposed with the V, W vector fields at a single time snapshot for the $k_x = 0$ (zero streamwise wave number) mode of the DNS (with a minimal streamwise channel $L_x = 1.2\pi$), the QL and the 2D/3C. A minimal channel was used in order to minimize any smoothing effects resulting from the implied streamwise averaging associated with the $k_x = 0$ mode of the DNS. For comparison, Figure 7 shows the same plot obtained from a DNS run in the longer channel (with $L_x = 4\pi$), where the effects of this averaging are much more evident. The qualitative features of the roll and streak structures depicted in Figures 6 and 7 are remarkably similar for all of the models discussed.

7. Conclusions and directions for future work

The 2D/3C model captures the dynamics of the interactions between the roll structures and the mean flow. It provides accurate statistics for the turbulent mean flow when stochastically forced at the appropriate amplitude. This result implies that the primary mechanism determining the structure of the turbulent mean flow is streamwise constant. One implication of this conclusion is that the mechanism producing the mean flow can be isolated from the mechanism maintaining the turbulent state and analyzed separately. However, understanding how the roll and streak structure is maintained in a statistical steady state requires a model that also includes feedback from the streamwise constant mean flow to the streamwise varying perturbation dynamics. The addition of this feedback is accomplished in the SSST formulation by means of a second order closure. The additional feedback mechanism in the SSST model allows it to capture the dynamics of transition to turbulence as well as the self sustaining process that maintains the turbulent state. In this work we tested the predictions of both the 2D/3C and the SSST model by comparing them to DNS data. The SSST was simulated by imposing the dynamical restrictions of SSST on a DNS code to emulate the SSST dynamics via a QL model. The

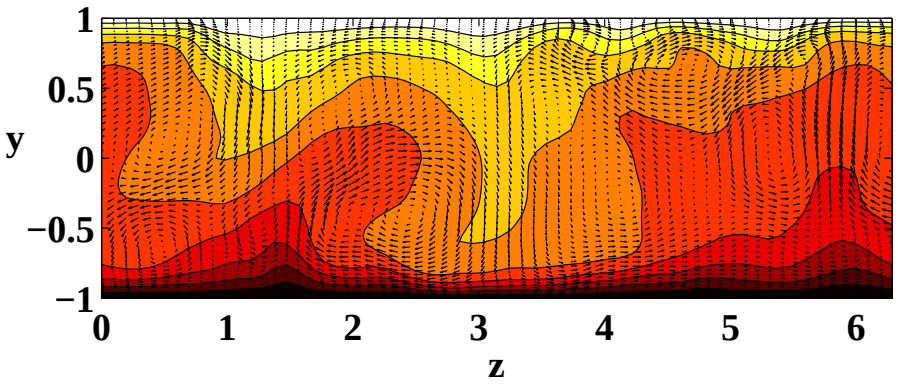

(a) DNS

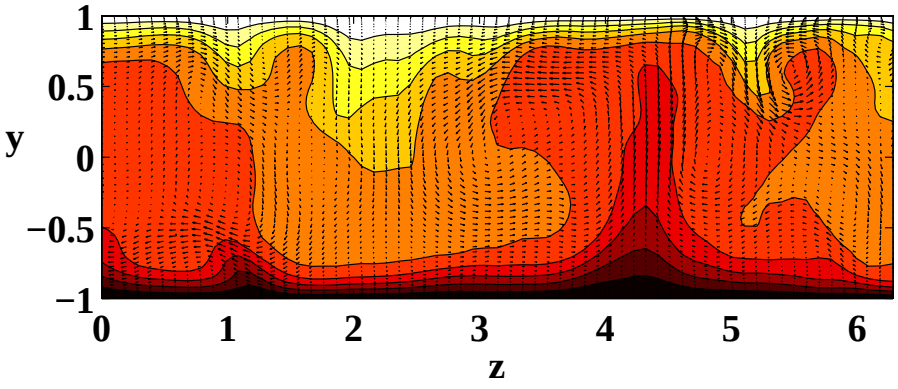

(b) QL

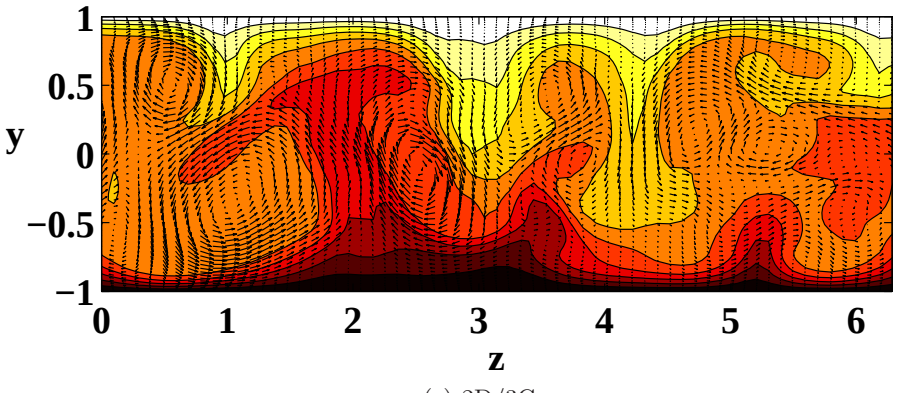

(c) 2D/3C

FIGURE 6. A y-z plane cross-section of the flow at a single snapshot in time (a) the $k_x = 0$ mode of the DNS, (b) the QL, and (c) the 2D/3C simulations, all at $R = 1000$. All panels show contours of the streamwise component of the mean flow U with the velocity vectors of (V, W) superimposed. The QL is self-sustaining ($f = 0$), and the 2D3C is forced with an amplitude $f = 0.065$.

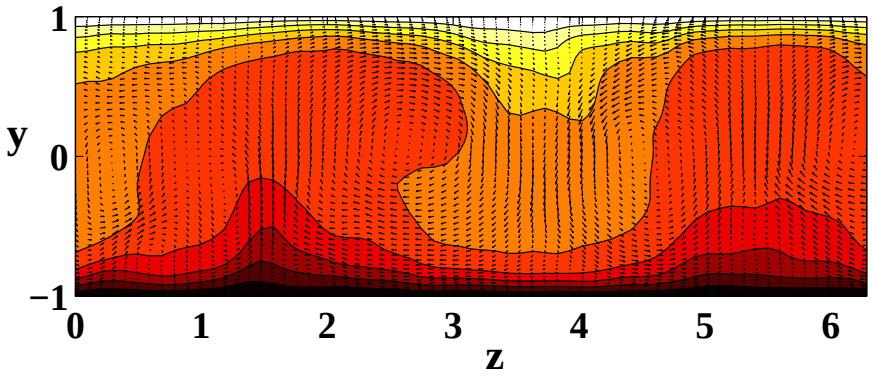

FIGURE 7. A $k_x = 0$ snapshot of the DNS with the longer ($L_x = 4\pi$) channel showing contours of the streamwise velocity field U with the velocity vectors of (V, W) superimposed. The averaging effect caused by the longer channel is clearly evident in the more regularized features versus the plots in Figure 6

results demonstrated good agreement between the 2D/3C, QL and DNS in the structure of the mean flow and mean perturbation statistics. The SSST based predictions for the behavior of the roll and streak structures during transition and the development of a self sustaining state was also verified by comparing the QL to DNS. These results imply that fundamental aspects of the dynamics of turbulence in plane Couette flow are streamwise constant (i.e. captured by the 2D/3C model). Also, further aspects, including transition and mechanisms associated with the self-sustaining process maintaining turbulence are contained in the extension to SSST. Moreover, because these dynamics are accurately captured by a maximally simple model that is dominated by one streamwise wave number interacting with the time-dependent streamwise mean flow, the results suggest that SSST provides a computationally tractable model system for further study of the dynamics of shear flow turbulence.

Acknowledgments

Part of this work was performed during the 2012 Center for Turbulence Research Summer Program with financial support from Stanford University and NASA Ames Research Center. We would like to thank Prof. P. Moin for his interest in our work and Prof. S. Lele for his useful comments that helped us improve quality of our presentation. Financial support from the National Science Foundation under CAREER Award CMMI-06-44793 (to M.R.J. and B.K.L.) and ATM-1246929 (to B.F.F) is gratefully acknowledged.

REFERENCES

ANDERSSON, P., BERGGREN, M. & HENNINGSON, D. S. 1999 Optimal disturbances and bypass transition in boundary layers. *Phys. of Fluids* **11**, 134–150.

CANUTO, C., HUSSAINI, M., QUATERONI, A. & ZHANG, T. 1988 *Spectral Methods in Fluid Dynamics*. Springer-Verlag.

FARRELL, B. & IOANNOU, P. 2012 Dynamics of streamwise rolls and streaks in turbulent wall-bounded shear flow. *J. Fluid Mech.* **708**, 149 –196.

GAYME, D. F. 2010 A robust control approach to understanding nonlinear mechanisms in shear flow turbulence. PhD thesis, Caltech, Pasadena, CA, USA.

Gayme, D. F., McKeon, B. J., Papachristodoulou, A., Bamieh, B. & Doyle, J. C. 2010 Streamwise constant model of turbulence in plane Couette flow. *J. Fluid Mech.* **665**, 99–119.

Gibson, J. F. 2012 Channelflow: A spectral Navier-Stokes simulator in C++. *Tech. Rep.*. U. New Hampshire, `Channelflow.org`.

Guala, M., Hommema, S. E. & Adrian, R. J. 2006 Large-scale and very-large-scale motions in turbulent pipe flow. *J. Fluid Mech.* **554**, 521–542.

Hamilton, J. M., Kim, J. & Waleffe, F. 1995 Regeneration mechanisms of near-wall turbulence structures. *J. Fluid Mech.* **287**, 317–348.

Hutchins, N. & Marusic, I. 2007*a* Evidence of very long meandering structures in the logarithmic region of turbulent boundary layers. *J. Fluid Mech.* **579**, 1–28.

Hutchins, N. & Marusic, I. 2007*b* Large-scale influences in near-wall turbulence. *Phil. Trans. Royal Soc. London A* **365**, 647–664.

Jiménez, J. & Moin, P. 1991 The minimal flow unit in near-wall turbulence. *J. Fluid Mech.* **225**, 213–240.

Jiménez, J. & Pinelli, A. 1999 The autonomous cycle of near-wall turbulence. *J. Fluid Mech.* **389**, 335–359.

Jovanović, M. R. & Bamieh, B. 2005 Componentwise energy amplification in channel flows. *J. Fluid Mech.* **534**, 145–183.

Kim, J., Moin, P. & Moser, R. 1987 Turbulence statistics in fully developed channel flow at low Reynolds number. *J. Fluid Mech.* **177**, 133–166.

Kim, K. J. & Adrian, R. J. 1999 Very large scale motion in the outer layer. *Phys. of Fluids* **11** (2), 417–422.

Klebanoff, P. S., Tidstrom, K. D. & Sargent, L. M. 1962 The three-dimensional nature of boundary-layer instability. *J. Fluid Mech.* **12**, 1–34.

Mathis, R., Hutchins, N. & Marusic, I. 2009 Large-scale amplitude modulation of the small-scale structures of turbulent boundary layers. *J. Fluid Mech.* **628**, 311–337.

Morrison, J. F., McKeon, B. J., Jiang, W. & Smits, A. J. 2004 Scaling of the streamwise velocity component in turbulent pipe flow. *J. Fluid Mech.* **508**, 99–131.

Peyret, R. 2002 *Spectral Methods for Incompressible Flows*. Springer-Verlag.

Zang, T. A. & Hussaini, M. Y. 1985 Numerical experiments on subcritical transition mechanism. In *AIAA, Aerospace Sciences Meeting*. Reno, NV.